PNAS
www.pnas.org

Supplementary Information for

Human Cytomegalovirus US21 Protein Is a Viroporin That Modulates Calcium Homeostasis and Protects Cells Against Apoptosis

Anna Luganini, Giovanna Di Nardo, Luca Munaron, Gianfranco Gilardi, Alessandra Fiorio Pla, and Giorgio Gribaudo

Department of Life Sciences and Systems Biology, University of Torino, 10123 Torino, Italy

Corresponding author: **Giorgio Gribaudo** Email: giorgio.gribaudo@unito.it

This PDF file includes:

Supplementary text
Figures S1 to S7
Table S1
References for SI reference citations

www.pnas.org/cgi/doi/10.1073/pnas.1813183115

Supplementary Information Text

Materials and Methods

Oligonucleotides. All oligonucleotides used for PCR, mutagenesis, and sequencing were obtained from Life Technologies. They are listed in Table S1.

Virus Recombineering. Recombinant HCMV TR derivatives containing modifications in the US21 gene (Fig. S1) were generated by a two-step replacement strategy using the *galK* recombineering method, as previously described (1, 2). In the first step, a *galK-kan* cassette was PCR-amplified from the pGalK-Kan plasmid (a gift from D. Yu) using the US21-*galK/kan* primer set (Table S1) and then electroporated into *E. coli* SW102 harboring the TR BAC (3, 4). Several Kan- and Gal-positive TRΔUS21 colonies were selected for US21 replacement by PCR and sequencing, and then used to start the counterselection step. To generate TRUS21HA BAC, TRUS21stop BAC, and TRUS21NV5-CHA BAC, the *galK-kan* cassette in TRΔUS21 BAC was replaced with the appropriate US21-modified gene cassette (generated with the primer sets shown in Table S1) as previously described (2). Kan- and Gal-negative colonies were then screened for the replacement of *galK-kan* sequences with modified versions of the US21 ORF by PCR, followed by restriction enzyme analysis and sequencing. Two independent TRΔUS21, TRUS21stop, TRUS21HA, and TRUS21NV5-CHA BAC clones were selected and characterized to ensure that their phenotypes did not result from an off-target mutation.
Infectious recombinant viruses (RV) TRΔUS21, TRUS21stop, TRUS21HA, TRUS21NV5-CHA, and TRwt were reconstituted in HFF cells by cotransfection of the corresponding BAC and a plasmid expressing HCMV pp71 (a gift from T. Shenk) using SuperFect Transfection Reagent (Qiagen). Transfected HFFs were then cultured until a marked cytopathic effect was observed. Viral stocks and viral titers were obtained as previously described (2, 5).

Antibodies. Detection of viral and cellular proteins by immunofluorescence was carried out using the following antibodies: the rat monoclonal antibody (MAb) anti-HA (clone 3F10, Roche); mouse MAbs against V5 (clone R960-25; Life Technologies); UL83 (pp65) (clone 3A12; Virusys); gB (clone CH28, Virusys); GM130 (clone 35/GM130; BD Biosciences); calreticulin (CALR) (clone 16/calreticulin; BD Biosciences); EEA1 (clone 14/EEA1; BD Biosciences), CD63 (sc-5275; Santa Cruz).
For immunoblotting, the following antibodies were used: mouse MAbs against IEA (IE1 plus IE2) (clone E13, Argene Biosoft); UL44 (clone CH16, Virusys); UL99 (pp28) (clone CH19, Virusys); and the rat anti-HA MAb conjugated to horseradish

peroxidase (clone 3F10, Roche). Immunodetection of tubulin with a mouse MAb (clone TUB 2.1, Sigma) was used as a control for cellular protein loading.

Immunofluorescence. Immunofluorescence analysis of viral antigens was performed as previously described (2, 6-8). For selective permeabilization assays (9), cells were treated with either 20 μM digitonin (Sigma-Aldrich) in KHM buffer (110 mM potassium acetate, 20 mM HEPES, 2 mM $MgCl_2$) for 4 min at 4°C to selectively permeabilize the plasma membrane, or with 0.1% Triton X-100 in KHM buffer for 5 min to permeabilize all cellular membranes, as previously described (8). The binding of primary antibodies was detected with CF594-conjugated rabbit anti-mouse IgG antibodies (Sigma) or with CF488A-conjugated rabbit anti-rat IgG (Sigma). Nuclei were counterstained with DAPI (4',6-diamidino-2-phenylindole) where indicated. Mitochondrial staining was performed by means of MitoTracker Red CMXRos (ThermoFischer Scientific).
Samples were then visualized with an Olympus IX50 fluorescence microscope equipped with Image pro-plus software. The intracellular localization of proteins was examined using an Olympus IX70 inverted laser scanning confocal microscope, and images were captured using FluoView 300 software (Olympus Biosytems). For quantitative colocalization of proteins, confocal microscopy images were analyzed to evaluate the Pearson's correlation coefficient by ImageJ as described by Adler and Parmryd (10).

qRT-PCR. Real-time reverse transcription (RT)-PCR analysis was performed on an Mx 3000 P (Stratagene) using SYBR green as a nonspecific PCR product fluorescent label as previously described (2, 11). Briefly, total cellular RNA was extracted from infected cells using the NucleoSpinRNAkit (Macherey-Nagel) and retrotranscribed using the RevertAid RT reverse transcription kit (Life Technologies). cDNAs (or water, as a control) were then amplified in triplicate by real-time RT-PCR using the SsoAdvanced™ Universal SYBR® Green Supermix (BioRad) in a final volume of 20 μl. Primer sequences for assessing IE1, UL32, UL44, UL99 and β-actin mRNA levels are listed in Table S1. The optimized cycling conditions were as follows: polymerase activaction and initial DNA denaturation at 95°C for 30 s, followed by 40 cycles of denaturation at 95°C for 15 s, primer annealing at 55°C for 1 min, and extension at 72°C for 1 min. For relative quantification analysis, semi-logarithmic plots were constructed of delta fluorescence versus cycle number and a threshold was set for the changes in fluorescence at a point in the linear PCR-amplification phase (C_t). The C_t values for each gene were normalized to the C_t values for endogenous β-actin reference using the ΔC_t equation. The level of target RNA, normalized to the gene reference, and relative to the TRwt 24h infected cells (calibrator sample), was calculated by the comparative C_t method with the $2^{-\Delta\Delta Ct}$ equation.

Statistical analysis. Results are expressed as the means and standard deviations (SD) for independent experiments. Data were analyzed for significance using

paired t-tests or one-way analysis of variance (ANOVA) with Bonferroni post-test correction for multiple comparisons. A p value ≤ 0.05 was considered significant. All statistical tests were performed using GraphPad Prism version 5.01 for Windows (GraphPad Software).

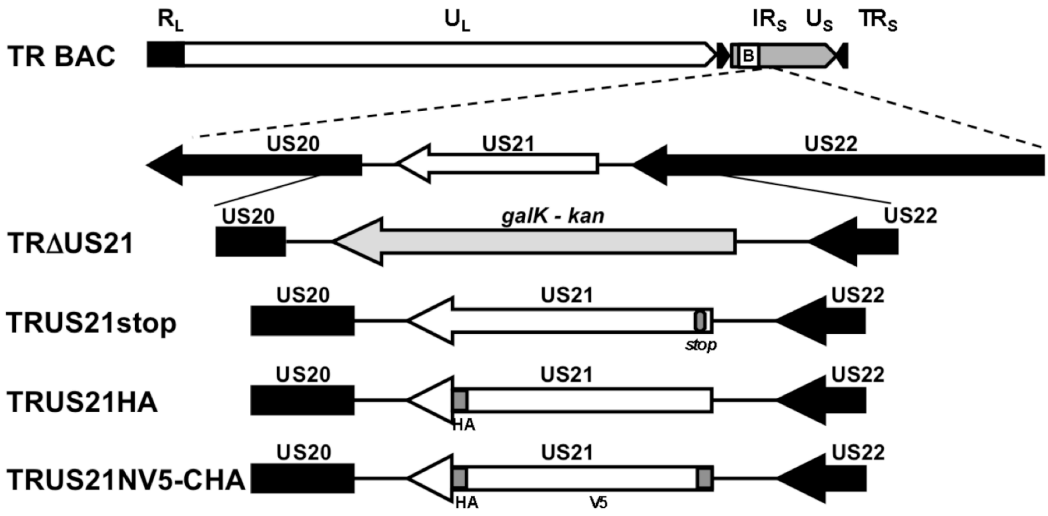

Fig. S1. Graphic representation of the HCMV US21 gene region and the modifications that were introduced into the ORF. In TRΔUS21, the US21 ORF was substituted with a cassette containing the *galK-kan* genes. In TRUS21stop a single nucleotide was changed in codon 8 of the US21 ORF. This change created a stop codon in the 8th codon, as well as a unique restriction site for *Xba1*. TRUS21HA was generated from TRΔUS21 by reintroducing the US21 ORF fused with the coding sequence for an HA epitope tag at its C terminus. TRUS21NV5-CHA was generated from TRΔUS21 by reintroducing the US21 ORF fused with the coding sequence for an HA epitope tag at its C terminus and a V5 epitope at its N terminus. Recombinant BACs were examined for the desired mutation by PCR and sequencing.

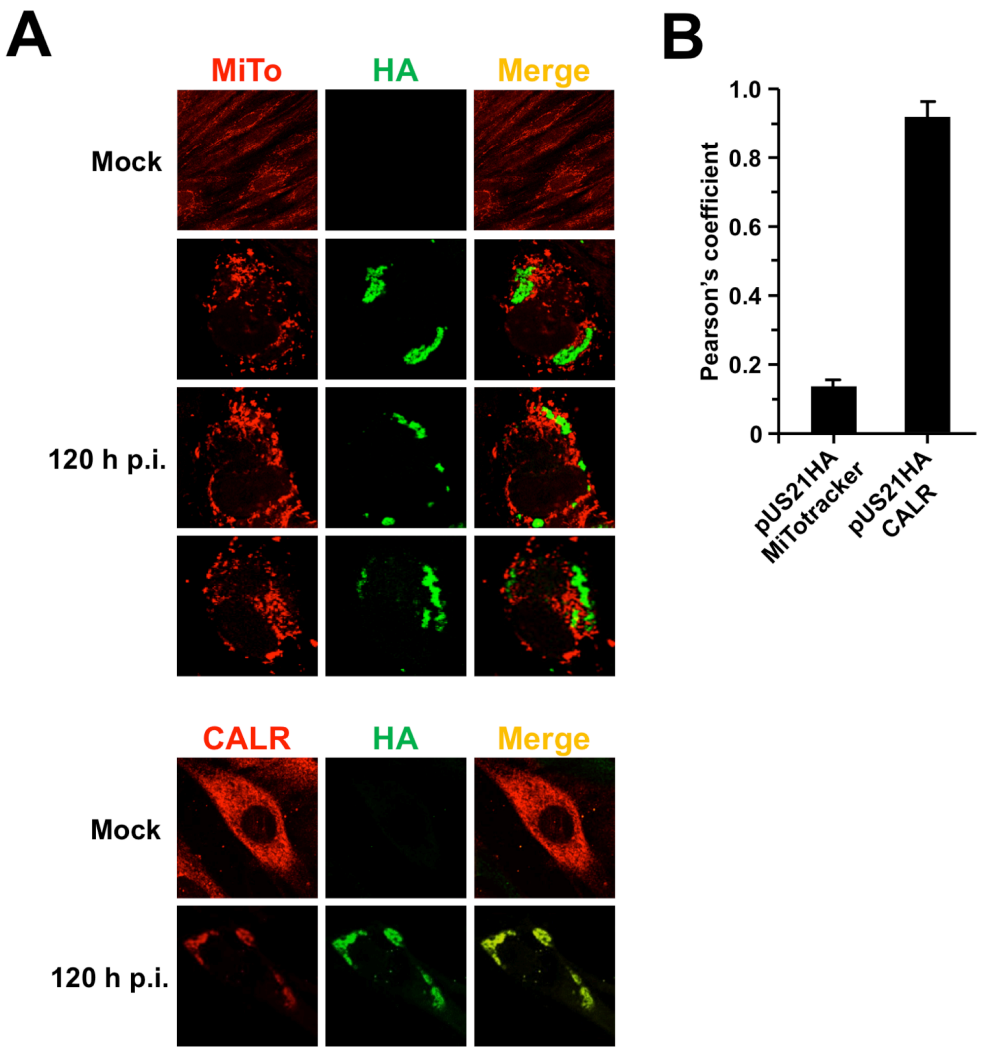

Fig. S2. Intracellular localization of pUS21HA. A) pUS21HA localizes in ER-derived membranes. HFFs were mock-infected or infected with TRUS21HA (MOI of 1 PFU/cell). At 120 h p.i., cell cultures were stained with MitoTracker Red CMXRos (MiTo) (a mitochondrial stain), and then fixed, permeabilized, and stained with antibodies against HA (green) (upper panel); as a control, cell samples were fixed, permeabilized, and stained with antibodies against HA (green) and calreticulin (CALR) (ER marker, red) (lower panel). Three representative images showing MiTotracker and HA staining of TRUS21HA-infected cells are shown in the upper panel. Images are representative of two independent experiments. **(B) Colocalization coefficients for pairs of viral and cellular organelle markers**. Pearson's correlation for colocalization of signals between pUS21HA and MitoTracker or CALR was determined in confocal microscopy images collected from cells infected with TRUS12HA for 120 h p.i. Ten randomly chosen fields were evaluated for each pair of makers. The data shown are the averages of two independent experiments ± SD.

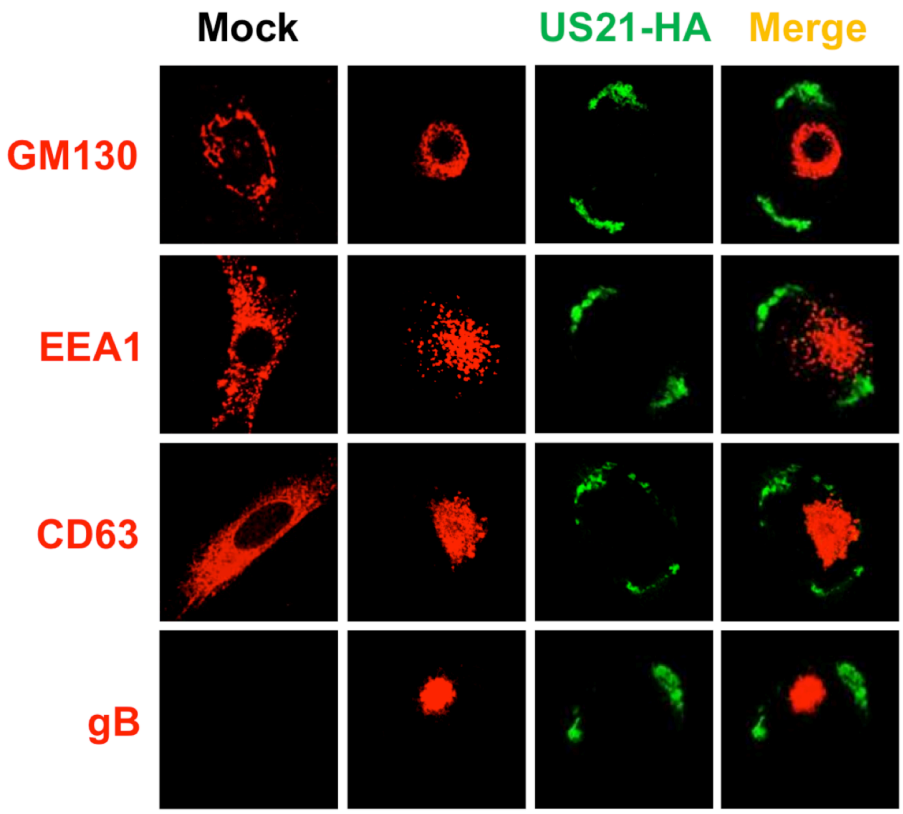

Fig. S3. pUS21HA does not accumulate in the cytoplasmic virion assembly compartment (cVAC) of HCMV-infected cells. HFFs were infected with TRUS21HA (MOI of 1 PFU/cell) or mock-infected. At 120 h p.i., the cells were fixed, permeabilized, and stained for pUS21HA (green) and for GM130 (Golgi marker), EEA1 (early endosomal marker), CD63 (late endosomal marker), and gB (red), which are all known to accumulate in the cVAC. Immunofluorescence experiments were repeated twice, and representative images visualized by confocal microscopy are presented. Magnification: x60.

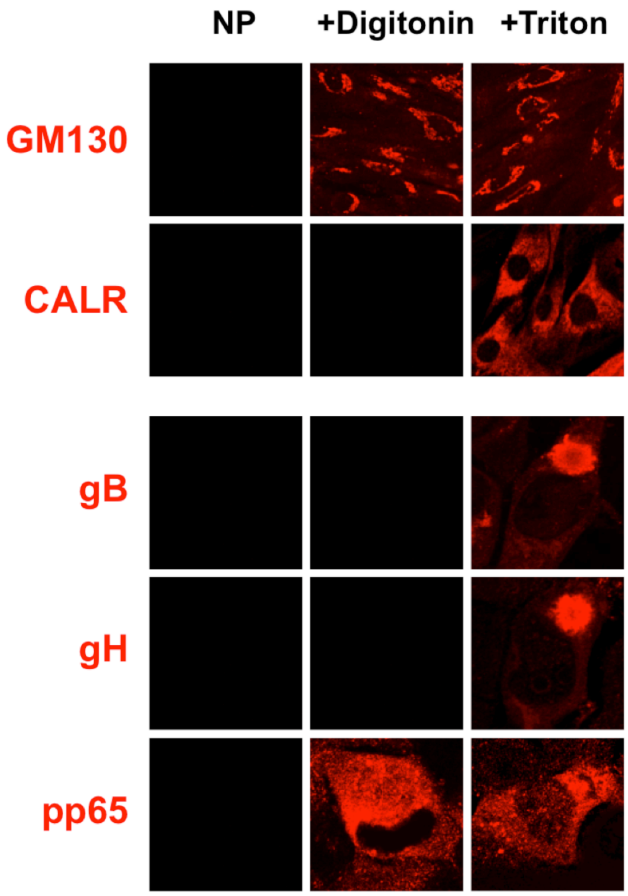

Fig. S4. Validation of selective permeabilization assay. HFFs were mock-infected or infected with TRUS21NV5-CHA (MOI of 1 PFU/cell), and at 120 h p.i., cells were not permeabilized (NP), or selectively or completely permeabilized using digitonin (+Digitonin) or Triton X-100 (+Triton). Then, mock-infected cells were stained with GM130 (as a cytoplasmic marker) and CALR (as a luminal marker), whereas HFFs infected with TRUS21NV5-CHA were stained with gB, gH (as luminal markers), and pp65 (as a cytoplasmic marker). Images are representative of three independent experiments. Magnification: x60.

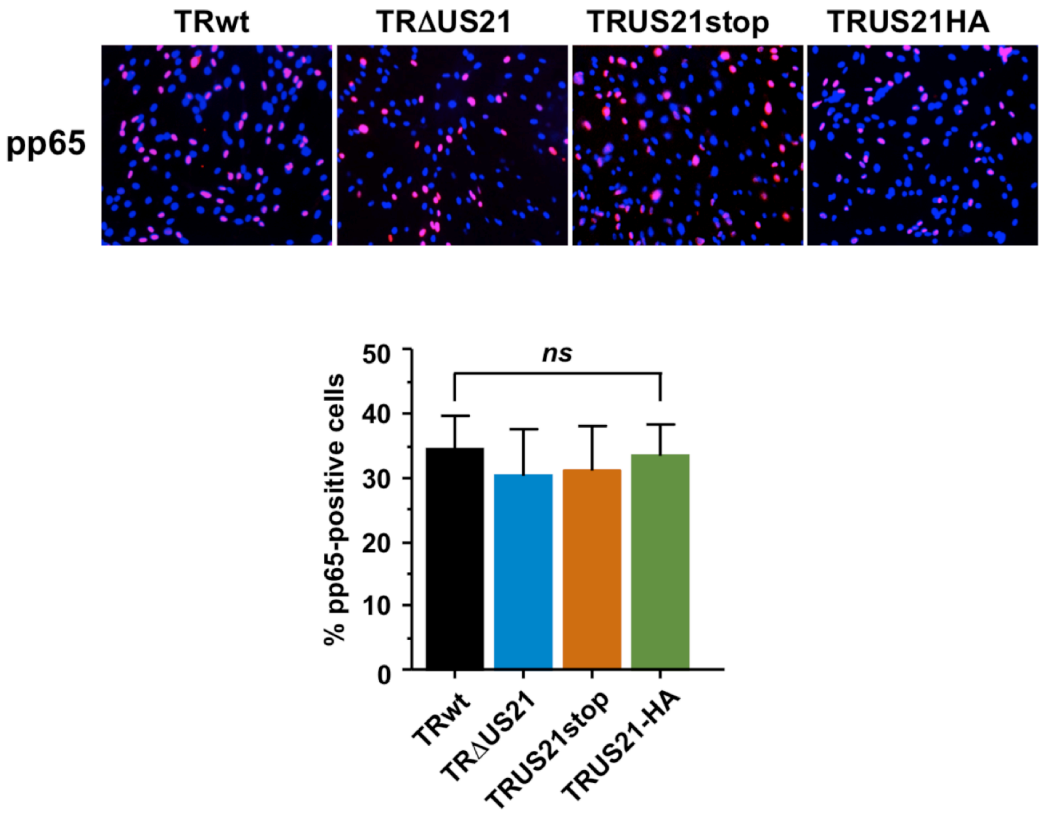

Fig. S5. Entry of US21-deficient viruses into fibroblasts. HFFs were infected with TRwt, TRΔUS21, TRUS21stop, and the revertant TRUS21HA (MOI of 1 PFU/cell). At 8 h p.i., the cells were fixed, permeabilized, and stained with an anti-UL83 (pp65) MAb. Fluorescent microscopy was used to quantify the percentage of pp65-positive cells in 20 different fields. Immunofluorescence experiments were repeated three times, and representative images are presented (magnification: x10).

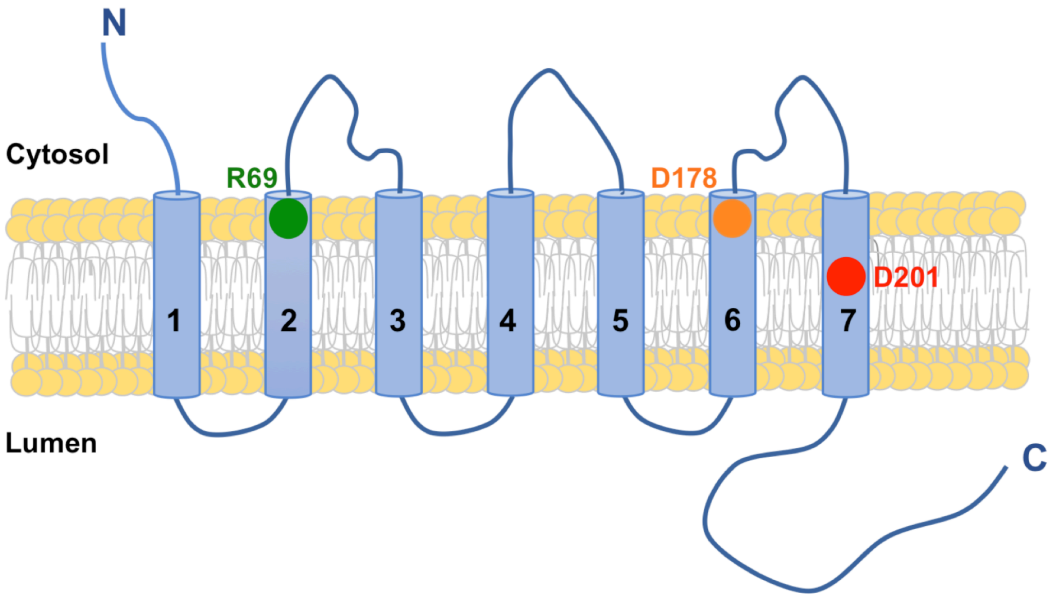

Fig. S6. Proposed topological 7TMDs structure of pUS21. The location of putative residues (Arg69, Asp178, and Asp20) of pUS21 corresponding to those previously shown to be important for channel activity of the related bacterial protein BsYetJ, are shown.

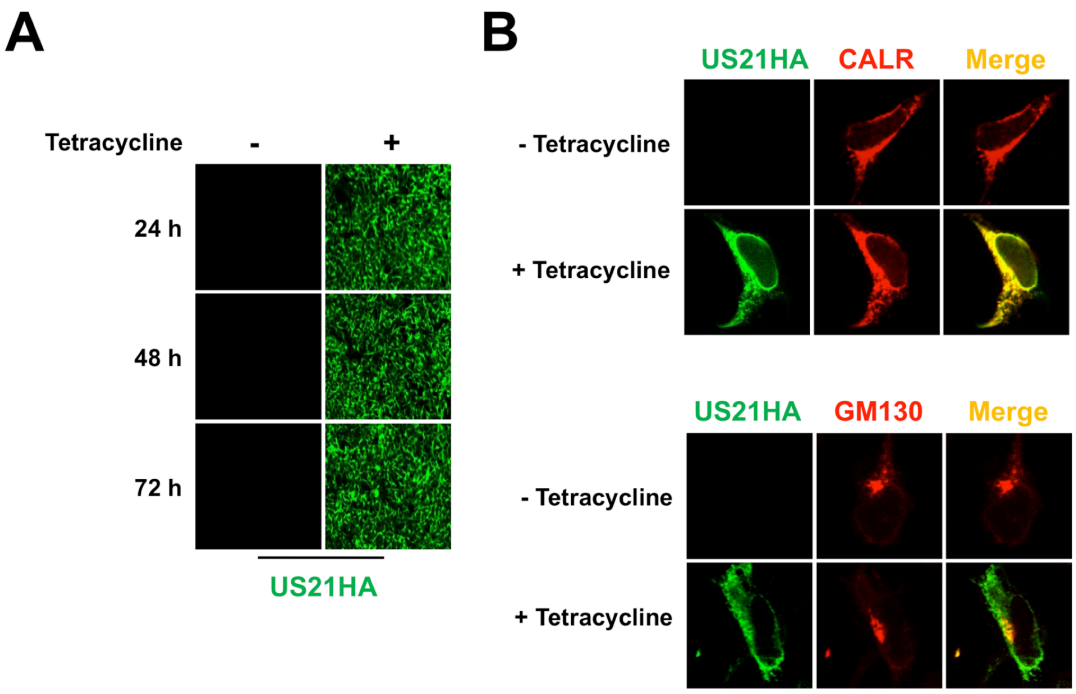

Fig. S7. Expression of pUS21HA. A) Tetracyclin-inducible expression of pUS21HA in TRex-293 cells. TRex-293-US21HA cells were treated with tetracycline (1 μg/ml) and at the indicated times the cells were fixed, permeabilized, and stained with an anti-HA MAb. Immunofluorescence experiments were repeated three times and representative images are presented (magnification: x10). **B) Intracellular location of the tetracyclin-inducible expression of pUS21HA in TRex-293 cells.** TRex-293-US21HA cells were treated with tetracycline (1 μg/ml) and at 48 h the cells were fixed, permeabilized, and immunostained with an anti-HA (green) and either GM130 (Golgi marker, red) or calreticulin (CALR) (ER marker, red) MAbs. Images are representative of three independent experiments. Magnification: x60.

Table S1. Oligonucleotides used for cloning, BAC mutagenesis, and PCR analysis.

Primer designation		Sequence 5' → 3' [(a)]
US21-*galK*/*kan*-F		CGCTTCGTGTATTTAGACGAATCTCGGCGATAACCGC CGGCGTTGCCGCCCCTGTTGACAATTAATCATCG
US21-*galK*/*kan*-R		CAAGCGAGCGAGTGGGGCACGGTGACGTGGTCACG CCGCGGACACGTCGACTCAGCAAAAGTTCGATTTA
US21-HA-F		ATGTCGCTCCGCGGTCAGG
US21-HA-R1		CTAAGCGTAGTCTGGGACGTCGTATGGGTATCCTCC TCCCTGAAAATACAGGTTTTCTCCTCCGGAGACGAA CTGGGGCGACG
US21-HA-R2		CAAGCGAGCGAGTGGGGCACGGTGACGTGGTCACG CCGCGGACACGTCGACTAAGCGTAGTCTGGGACGTC
US21-stop-F		CGCTTCGTGTATTTAGACGAATCTCGGCGATAACCGC CGGCGTTGCCGCCATGTCGCTCCGCGGTCAGG**tc tag a**TAGCCCGGTCG
US21-stop-R		CAAGCGAGCGAGTGGGGCACG
US21-NV5-F1		GGCGTTGCCGCCATGGGTAAGCCAATCCCTAACCCG CTCCTAGGTCTTGATTCTACGTCGCTCCGCGGTCAG GTCC
US21-NV5-F2		CGCTTCGTGTATTTAGACGAATCTCGGCGATAACCGC CGGCGTTGCCGCCATGGGTAAG
US21-D178N	forward	ACCTCGGTGGTGTGCAACACGCAGGACATCCTG
	reverse	CAGGATGTCCTGCGTGTTGCACACCACCGAGGT
US21-D201N	forward	CGCTCTGCTTGTACATGAACCTCATGTACCTCTTT
	reverse	AAAGAGGTACATGAGGTTCATGTACAAGCAGAGCG
IE1 mRNA	forward	CACGACGTTCCTGCAGACTA
	reverse	TTTTCAGCATGTGCTCCTTG
UL44 mRNA	forward	GTGGAAACTGACGCGGTTAT
	reverse	ATCTAGATTTCGGCGTGGTG
UL99 mRNA	forward	GTGTCCCATTCCCGACTCG
	reverse	TTCACAACGTCCACCCACC
UL32 mRNA	forward	GGCGCGGGAACCTCTT
	reverse	CCGTGGGCGACAAAACG
β-actin mRNA	forward	GTTGCTATCCAGGCTGTG
	reverse	TGTCCACGTCACACTTCA

[(a)] Lowercase boldface letters indicate restriction enzyme sites.

References

1. Warming S, Costantino N, Court DL, Jenkins NA, Copeland NG (2005) Simple and highly efficient BAC recombineering using galK selection. *Nucleic Acids Res* 33: e36.

2. Cavaletto N, Luganini A, Gribaudo G (2015) Inactivation of the human cytomegalovirus US20 gene hampers productive viral replication in endothelial cells. *J Virol* 89:11092-11106.

3. Smith IL, Taskintuna I, Rahhal FM, Powell HC, Ai E, Mueller AJ, Spector SA, Freeman WR (1998) Clinical failure of CMV retinitis with intravitreal cidofovir is associated with antiviral resistance. *Arch Ophthalmol* 116: 178–185.

4. Murphy E, Yu D, Grimwood J, Schmutz J, Dickson M, Jarvis MA, Hahn G, Nelson JA, Myers RM, Shenk T (2003) Coding potential of laboratory and clinical strains of human cytomegalovirus. *Proc Natl Acad Sci U S A* 100: 14976–14981.

5. Luganini A, Cavaletto N, Raimondo S, Geuna S, Gribaudo G (2017) Loss of the human cytomegalovirus US16 protein abrogates virus entry into endothelial and epithelial cells by reducing the virion content of the pentamer. *J Virol* 91: e00205-17.

6. Brune W, Nevels M, Shenk T (2003) Murine cytomegalovirus m41 open reading frame encodes a Golgi-localized antiapoptotic protein. *J Virol* 77: 11633–11643.

7. Das S, Vasanji A, Pellet PE (2007). Three-dimensional structure of the human cytomegalovirus virion assembly complex includes a reoriented secretory apparatus. *J Virol* 81: 11861-11869.

8. Das S, Pellet PE (2011) Spatial relationships between markers for secretory and endosomal machinery in human cytomegalovirus-infected cells versus those in uninfected cells. *J Virol* 85: 5864-5879.

9. Carrara G, Saraiva N, Gubser C, Johnson BF, Smith GL (2012) Sixtransmembrane topology for Golgi anti-apoptotic protein (GAAP) and Bax inhibitor 1 (BI-1) provides model for the transmembrane Bax inhibitor containing motif (TMBIM) family. *J Biol Chem* 287: 15896–159.

10. Adler J, Parmryd I (2013) Colocalization analysis in fluorescence microscopy. *Meth Mol Biol* 319: 97-109.

11. Caposio P, Luganini A, Bronzini M, Landolfo S, Gribaudo G (2010) The Elk-1 and Serum Response Factor binding sites in the Major Immediate-Early promoter of human cytomegalovirus are required for efficient viral replication

in quiescent cells and compensate for inactivation of the NF-κB sites in proliferating cells. *J Virol* 84: 4481-4493.